Ocean Engineering 213 (2020) 107709

Contents lists available at ScienceDirect

Ocean Engineering

journal homepage: www.elsevier.com/locate/oceaneng

Determination of the dynamic critical maneuvering area in an encounter between two vessels: Operation with negligible environmental disruption

Mateusz Gil [a,b,*], Jakub Montewka [a,b], Przemyslaw Krata [a,c], Tomasz Hinz [b], Spyros Hirdaris [b]

[a] Gdynia Maritime University, Research Group on Maritime Transportation Risk and Safety, Morska 81-87, 81-225, Gdynia, Poland
[b] Aalto University, Department of Mechanical Engineering, Marine Technology, P.O. Box 15300, FI-00076, Aalto, Finland
[c] Waterborne Transport Innovation, 83-050, Lapino, Poland

ARTICLE INFO

Keywords:
Collision avoidance dynamic critical area (CADCA)
Evasive maneuver
Maritime risk and safety
Ship maneuvering area
Last-minute maneuver (LMM)
COLREGs

ABSTRACT

This paper introduces the concept of *Collision Avoidance Dynamic Critical Area* (CADCA) for onboard *Decision Support Systems* (DSS). The indicator proposed is derived via identification of a minimum required maneuvering zone in an encounter between two vessels. The CADCA model accounts for ship maneuvering dynamics and associated hydrodynamic actions emerging from different rudder angles and forward speed effects. The method presented is novel as it considers the variability of a critical area due to dynamic changes in operational parameters for both vessels. Results of the simulations carried out in negligible weather conditions confirm that computed zones may differ significantly in terms of shapes and limits. It is demonstrated that the size of the CADCA depends on the rudder angle, forward speed, as well as the dimensions of the vessels.

1. Introduction

The emergence of novel ship designs, technologies, and concepts implies the clear and compelling need to equip ship navigators and personnel involved with ship operations ashore with modern, proven tools that are optimized for good decision support. Such navigation systems should enhance safe and technologically sustainable ship operations i.e. should help to improve safety standards and reduce human error in scenarios involving ship encounters in conditions of traffic congestion, remoteness or autonomy.

Nowadays, the most common indicators used to examine a potential collision threat in an encounter between two vessels are the CPA (*Closest Point of Approach*) and TCPA (*Time to Closest Point of Approach*). These are utilized in the ARPA (*Automatic Radar Plotting Aid*), which is a mandatory piece of equipment for many vessels operating under the SOLAS Convention (*International Convention for the Safety of Life at Sea*), (IMO, 2014). The data of the acquired target is derived from the past observations of its motion. Moreover, the indicators presented in the ARPA do not directly translate into the parameters of the evasive maneuver, and so they require further elucidation by the OOW (*Officer of the Watch*). Various concepts on the graphical interpretation of ship vectors emerging from the ARPA are presented in literature on the subject (Bole et al., 2014). Those suggest more intuitive information for OOWs. For example, the PPC (*Potential Point of Collision*) and PAD (*Predicted Area of Danger*) are commonly used by operators of shipborne radars. The latter evolved over the years and transformed from circles to ellipses or polygons (Riggs, 1975; Riggs and O'Sullivan, 1980; Zhao-lin, 1988). Another concept known as *Collision Threat Parameters* (CTPs) was introduced and developed by Lenart (2015), 1983. To date CTPs have been utilized, modified, and validated by various researchers. For instance, Szlapczynski (2008); Szlapczynski and Smierzchalski (2009), combined CTP with fuzzy logic, while Szlapczynska and Szlapczynski (2017); Szlapczynski and Krata (2018); Szlapczynski and Szlapczynska (2017) applied it to the ship domains. Smierzchalski (2005), as well as Smierzchalski and Michalewicz (2000) utilized the concept in evolutionary path planning, whereas Chen et al. (2019), 2018 used a similar approach in probabilistic risk analyses.

Despite the progress made, the vast majority of existing solutions do not account for the influence of the dynamics of ship operations in a realistic environment. Accordingly, the number of studies focused on close-quarter situations considering ship dynamics has been limited (Colley et al., 1983; Hilgert, 1983; Krata et al., 2016; Montewka et al., 2012; Ni et al., 2019). However, the impact of weather conditions on an encounter between two vessels has been taken into account by Szlapczynski et al. (2018a), as well as Szlapczynski and Krata (2018). It is broadly acknowledged that ship operational parameters interpreted as rudder angle and initial forward speed may differ depending on the

* Corresponding author. Gdynia Maritime University, Department of Navigation, Jana Pawla II 3, 81-345, Gdynia, Poland.
E-mail address: m.gil@wn.umg.edu.pl (M. Gil).

https://doi.org/10.1016/j.oceaneng.2020.107709
Received 3 February 2020; Received in revised form 23 May 2020; Accepted 25 June 2020
Available online 10 August 2020

Abbreviations

6DoF	Six degrees of freedom
AIS	Automatic Identification System
ARPA	Automatic Radar Plotting Aid
BBN	Bayesian Belief Networks
CADCA	Collision Avoidance Dynamic Critical Area
COLREG	International Regulations for Preventing Collisions at Sea
CPA	Closest Point of Approach
CTP	Collision Threat Parameter
DSS	Decision Support System
ECDIS	Electronic Chart Display and Information System
EMSA	European Maritime Safety Agency
FSA	Floodstand-A Ship,
FSB	Floodstand-B Ship,
GNSS	Global Navigation Satellite System
IMO	International Maritime Organization
ITTC	International Towing Tank Conference
LMM	Last-minute maneuver
MASS	Maritime Autonomous Surface Ships
MDTC	Minimum Distance to Collision
OOW	Officer of the Watch
OS	Own ship
PAD	Predicted Area of Danger
PCC	Potential Point of Collision
PIANC	World Association for Waterborne Transport Infrastructure
PMM	Planar Motion Mechanism
SOLAS	International Convention for the Safety of Life at Sea
TCPA	Time to Closest Point of Approach
TS	Target ship
EU	European Union

encounter. Therefore, the maneuvering area should also vary to provide adequate prediction in real-time assessment. Its shape could respond to the influence of ship dynamics and operational conditions (Gil et al., 2019a, 2020a).

This idea of introducing a zonal indicator aligns with the priorities of the *e-Navigation* initiative introduced by the *International Maritime Organization* (IMO, 2008). The primary objective of this concept was to boost the level of maritime safety. This enhancement could be achieved *inter alia* by utilizing navigational DSSs (Gil et al., 2020b; Perera et al., 2015, 2012; Weintrit, 2013), especially for collision avoidance (Baldauf et al., 2014; Baldauf and Hong, 2016). Nevertheless, despite the progressive development of technological solutions implemented on merchant ships, a collision still remains one of the most common reasons for maritime disasters. In European waters, collisions comprise almost one quarter of navigational causes of accidents, while these represent more than half of all casualty events (EMSA, 2018). Therefore, providing new and effective methods of ship collision avoidance is essential. They could be utilized as a graphical form with a ship vector presented as an overlay to already existing onboard devices, like RADAR (Ma et al., 2015), or ECDIS (*Electronic Chart Display and Information System*), (Weintrit, 2009). Furthermore, experts with seagoing experience have evaluated the utilization of navigational equipment as essential in the process of ship-ship collision avoidance (Gil et al., 2019b).

This paper introduces the concept of *Collision Avoidance Dynamic Critical Area* (CADCA) as a novel safety zone that varies depending on the operational parameters of particular vessels. A version dedicated to onboard applications is presented here, so the target ship maintains her course and speed during an encounter. Consequently, the paper demonstrates an efficient method for determining CADCA in various simulation scenarios. Thirdly, it presents the application of the method in order to verify whether and how the operating parameters of the ship affect the required maneuvering area. Therefore, for the scenarios presented in this paper, the presence of wind and waves has been omitted.

The rest of the paper is organized as follows: the methods used in the study are presented in Section 2, along with assumptions, principles and a novel algorithm to determine CADCA. Section 3 provides an analysis of the results for various operational ship parameters in different simulation scenarios. The discussion about the presented solution and the methods used to handle uncertainties is provided in Section 4, while Section 5 concludes the paper.

2. Methods

The main intention of introducing a novel type of safety zone in the encounter between two vessels is twofold. Firstly, the required maneuvering area for evasive action should be determined for the most critical navigational scenarios. Secondly, the dynamics of a vessel in the process of collision avoidance should be taken into account to keep further reasoning realistic. The CADCA concept helps to define a minimum distance between encountering vessels which represents the last chance to avoid a collision. The own ship is located within the limits of the CADCA envelope that changes shape accordingly to the vessel's current operating parameters. In this paper the indicator related to the execution of an evasive maneuver and a 6DoF motion model have been used to determine the CADCA shape and its boundaries in realistic collision scenarios.

2.1. The last-minute maneuver (LMM)

The concept of CADCA is based on a critical navigational scenario known as the *last-minute* (also *-chance* or *-moment*) *maneuver*. This type of evasive action is strictly related to the requirements of the COLREGs (*International Regulations for Preventing Collisions at Sea*) Rule 17 (IMO, 2010). Several elaborations concerning the action of a stand-on vessel and interpretation of this regulation can be found in the literature, see e.g. (Cockcroft and Lameijer, 2012; Crosbie, 2008; Rymarz, 2007; Sweeney, 1992). However, only a few research papers related to LMM and especially its determination exist (Koszelew and Wołejsza, 2017; Miloh, 1975; Montewka and Krata, 2014; Ożoga and Montewka, 2018; Rymarz, 2007; Szlapczynski et al., 2018b).

According to COLREG Rule 17, the conduct of a stand-on vessel varies during an encounter situation (IMO, 2010). As shown in Fig. 1, an encounter of vessels approaching on collision courses can be divided

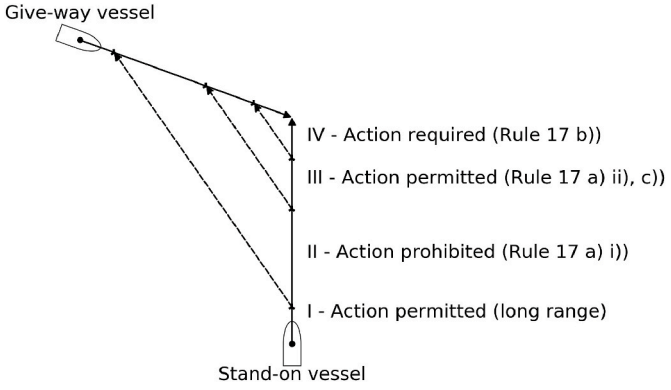

Fig. 1. Four stages of crossing encounter under the COLREGs Rule 17 considered from the perspective of the stand-on vessel, inspired by Cockcroft and Lameijer (2012); Rymarz (2007).

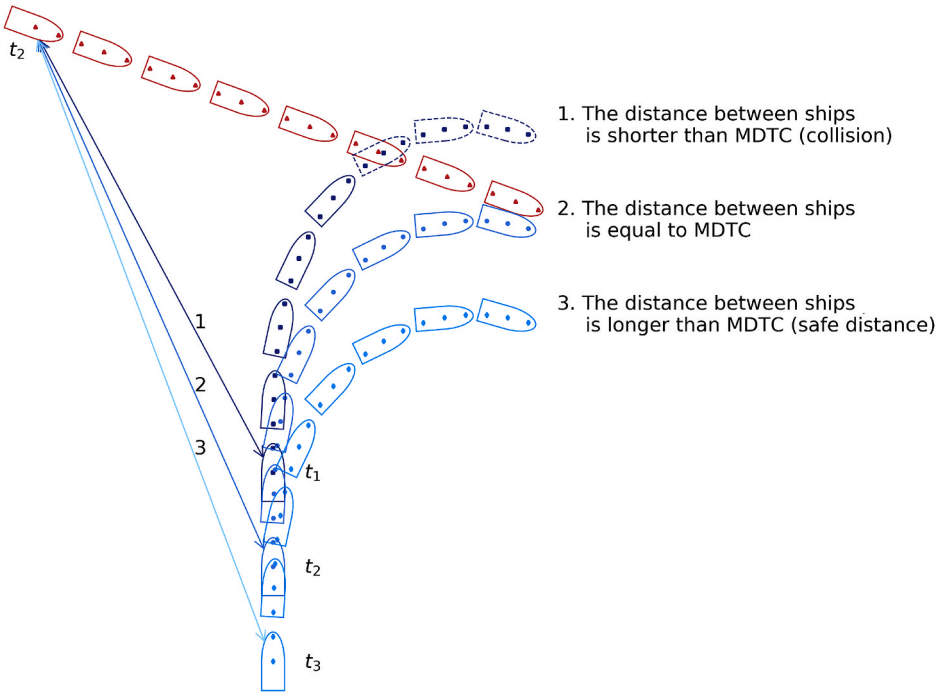

Fig. 2. Relations between MDTC and other distances in a ship encounter.

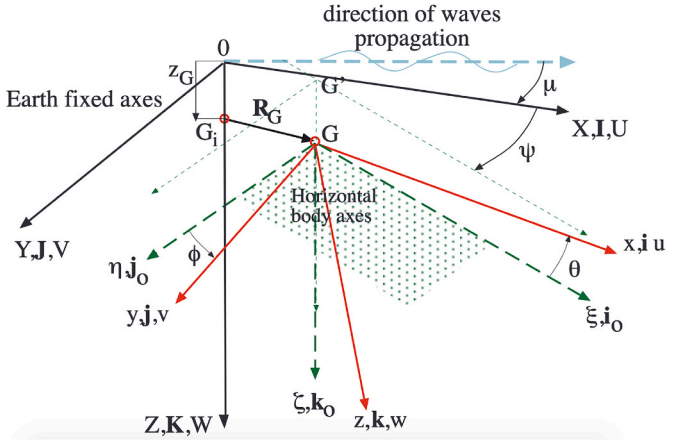

Fig. 3. Coordinate systems used in the LaiDyn model as in Matusiak (2017).

into four stages, where the ship's action depends on the distance between herself and the give-way vessel (Cockcroft and Lameijer, 2012; Rymarz, 2007). LMM refers to a situation when the stand-on vessel, despite the right of the way, is obliged to execute an evasive maneuver. That situation occurs if the action of the give-way vessel is executed too late or not undertaken at all. Therefore, the stand-on vessel is in stage IV and under Rule 17 her evasive action is mandatory. In such a situation, only effective single action undertaken by the stand-on vessel or joint operation involving both ships could avoid a collision.

Koszelew and Wołejsza (2017), as well as Wójcik et al. (2016) define LMM as a joint maneuver of both ships involved in an encounter, when the single action of the stand-on vessel would be insufficient to avoid a collision. This approach is fully compliant with the COLREG Rule 17 b), but from the operational point of view, a situation when the stand-on vessel has to execute a maneuver on her own seems to be even more essential. This is because of a lack or incorrect action of the give-way ship, which results in a larger maneuvering area being required. Therefore, in this paper the target vessel stays passive and maintains her present course and speed throughout the entire encounter.

2.2. Minimum Distance to Collision (MDTC)

In the CADCA concept, MDTC has been utilized since it allows to convert the distance in an encounter between two vessels into the required maneuvering area. MDTC was introduced by (Montewka et al., 2010) and further developed by (Montewka et al., 2012, 2011a; 2011b). As depicted in Fig. 2, this indicator can be defined as the minimum distance between two vessels in a close-quarters situation when the execution of successful evasive maneuver is still feasible. Therefore, MDTC allows for the determination of the LMM parameters.

MDTC is based on a two-dimensional coordinate system, where the projections of the vessels are plotted. Interpretation of their positions and headings may lead to the conclusion that in each encounter between two ships, only one MDTC exists. The indicator is calculated between the hulls for a given bearing and may take the hydrodynamics of the vessels into consideration. To this end, this paper uses ship trajectories projected by *LaiDyn* software.

2.3. The LaiDyn model

LaiDyn is a numerical ship motion model introduced by (Matusiak, 2017). It simulates the behavior of a vessel in regular and irregular waves, while also allowing for the combination of seakeeping and maneuvering (Acanfora et al., 2017; Matusiak, 2007, 2011). The ship is represented as a rigid body wherein non-linear wave effects, as well as restoring and Froude-Krylov forces, are included (Manderbacka et al., 2011).

The numerical model can be defined as a hybrid non-linear model in 6 degrees of freedom (6DoF) in the time domain with the assumption that the ship is a rigid body. The prime coordinate systems used for describing ship motion are presented in Fig. 3. To these belong the inertial system fixed to Earth with the X–Y plane coincident with the still water level, and the body-fixed reference frame (x, y, z) originating from the ship's center of gravity (Matusiak, 2017).

The equations of the motion in the time domain (1) are as follows (Matusiak, 2017):

$$
\begin{aligned}
&(m+a_{11})\dot{u}+a_{15}\dot{q}=-mg\sin\theta+X_{resistance}+X_{prop}+X_{rudder}+X_{wave}+X_{man}-k_{15}+(m+a_{22})(rv-qw)\\
&(m+a_{22})\dot{v}+a_{24}\dot{p}+a_{26}\dot{r}=mg\cos\theta\sin\varphi+(m+a_{11})(pw-ru)+Y_{man}+Y_{rudder}+Y_{wave}-k_{22}-k_{24}-k_{26}\\
&(m+a_{33})\dot{w}+a_{35}\dot{q}=mg\cos\theta\cos\varphi+m(uq-vp)+Z_{wave}-k_{33}-k_{35}\\
&a_{42}\dot{v}+(I_x+a_{44})\dot{p}+a_{46}\dot{r}=(I_y-I_z)qr-Y_{rudder}z_{rudder}+K_{man}+K_{wave}-k_{44}-k_{42}-k_{46}+2\zeta p\omega_{\varphi}\\
&a_{15}\dot{u}+a_{53}\dot{w}+(I_y+a_{55})\dot{q}=(I_y-I_x)pr+X_{rudder}x_{rudder}+M_{wave}-k_{55}-k_{53}-k_{15}\\
&a_{62}\dot{v}+a_{64}\dot{p}+(I_z-a_{66})\dot{r}=(I_x-I_y)pq+Y_{rudder}x_{rudder}+N_{man}+N_{wave}-k_{66}-k_{62}-k_{64}
\end{aligned}
\tag{1}
$$

Where m is ship mass, a_{ij} and k_{ij} are the added mass coefficients for infinite frequency and elements of the memory function, p, q, r, u, v, w are velocities (angular and linear), I_i are the mass moments of inertia; *resistance*, propulsion (*prop*), *wave*, and maneuvering (*man*) correspond to particular forces and moments acting on ship (Matusiak, 2017). The adopted notation uses the upper case letters for forces and moment components and the lower case letters for co-ordinates.

The stripe theory is applied to obtain the values of elements of the added mass matrix. We utilize *Sealoads* software (Kukkanen, 1995), although any other relevant method might be used.

The radiation and diffraction forces are calculated using the linear model, based on the assumption of small amplitude oscillatory motions (Journée and Massie, 2001; Kukkanen, 1995). Determining radiation forces, one takes into account the history of the past motions by applying the convolution integral representation (Cummins, 1962), see Equation (2).

$$
X_{rad}(t)=-a_{\infty}\ddot{x}(t)-\int_{-\infty}^{t}k(t-\tau)\dot{x}(\tau)d\tau \tag{2}
$$

Where a_{∞} is the matrix of added masses for an infinite frequency, x is response vector, k is the retardation function (also called *memory function*), which depends on a damping matrix (Cummins, 1962), τ is the time since the impulse initiation, whose contribution is modeled by the impulse function while t is the time instant at which the motion is computed. The convolution integral functions are used for heave, roll and pitch motions only.

The non-linear part of the code includes Froude-Krylov, hydrostatic forces, as well as maneuvering and propulsion (Manderbacka et al., 2011; Matusiak, 2011). The maneuvering part of the model is described as presented in Equation (3):

$$
\begin{aligned}
&X'=X'_{vv}v'^2+X'_{rr}r'^2+X'_{vvvv}v'^4\\
&Y'=Y'_{v}v'+Y'_{r}r'+Y'_{vv}v'|v'|+Y'_{rr}r'|r'|+Y'_{vvv}v'^3+Y'_{rrr}r'^3+Y'_{rrv}r'^2v'+Y'_{rvv}v'^2r'\\
&N'=N'_{v}v'+N'_{r}r'+N'_{vv}v'|v'|+N'_{rr}r'|r'|+N'_{vvv}v'^3+N'_{rrr}r'^3+N'_{rrv}r'^2v'+N'_{rvv}v'^2r'
\end{aligned}
\tag{3}
$$

Where v' and r' are sway and yaw velocities in the non-dimensional form defined as follows:

$v'=v/U$ and $r'=rL_{pp}/U$, with v sway velocity, U ship initial velocity, r yaw velocity and L_{pp} ship length between perpendiculars.

As given in the formulas (Equations (1)–(3)), the LaiDyn model utilizes a set of differential equations of motion, which implies a need for solving discrete-time equations. The Runge-Kutta methods are adopted in the software, which is quite a common approach.

LaiDyn has been validated by international benchmark studies (ITTC, 2005, 2002) and PMM (*Planar Motion Mechanism*) model tests (Matusiak and Stigler, 2012). The results demonstrated sufficient accuracy, especially for Ro-Paxes and container vessels (Acanfora et al., 2017), operating also in severe weather (Acanfora et al., 2018). Additionally, LaiDyn has been used in the estimation of dynamic effects of passenger ship flooding (Manderbacka et al., 2011), weather-routing of merchant vessels (Krata and Szlapczynska, 2018), as well as in a risk assessment and collision-avoidance (Hinz et al., 2018; Montewka et al., 2010; Szlapczynski et al., 2018a; Szlapczynski and Krata, 2018).

In the concept of CADCA, LaiDyn is utilized to simulate ship motions in 6DoF for specific operating and environmental conditions. The software generates vessel trajectories, including turning circles for various operational parameters. As a result, the ship's coordinates and values of her translational and rotational motions are delivered.

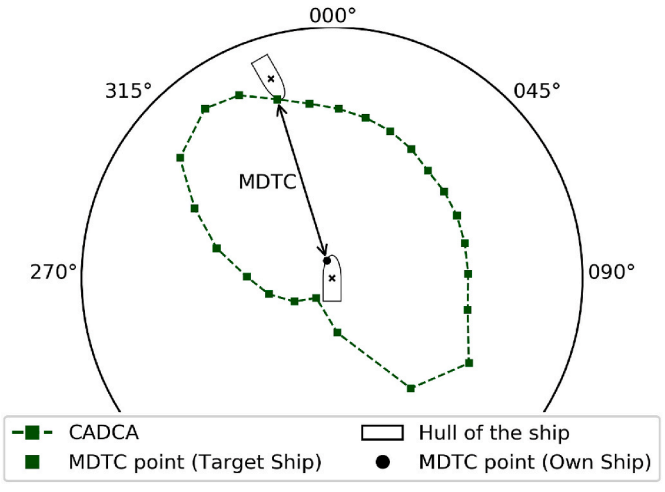

Fig. 4. The structure of CADCA.

2.4. CADCA structure

Previous studies introduced a simplified critical area for the case of a Ro-Pax vessel (Krata et al., 2016; Montewka and Krata, 2014). In this paper, the model and the method have been significantly improved by taking into account ship dynamics. CADCA shown in Fig. 4 is designed as a safety zone surrounding the ship in a close-quarters situation. The shape and limits of the envelope are delimited by MDTC values and the area can be generated for different navigational scenarios. These can include cases where one of the vessels involved in the encounter undertakes the single action or if they both act jointly. The ships can alter their courses to port or starboard side at various initial speeds using different settings of the rudder. Nevertheless, the OOW does not know

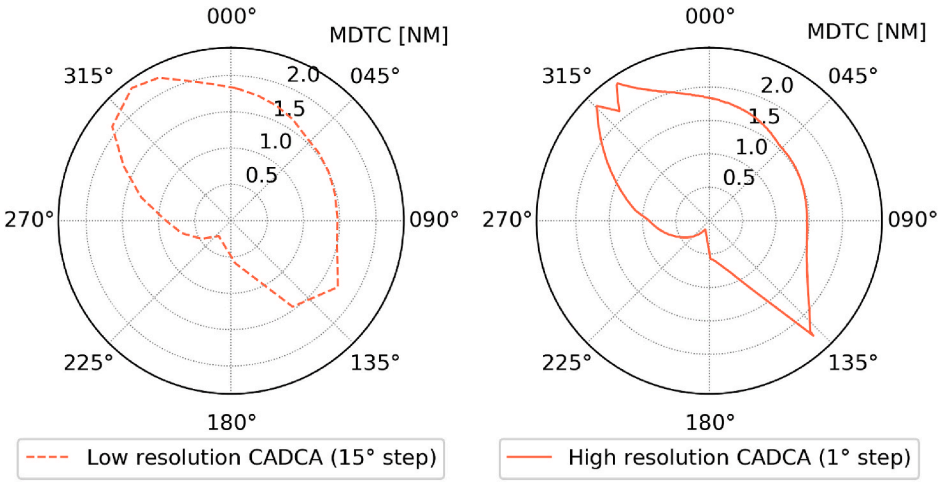

Fig. 5. The accuracy of CADCA in low (left) and high (right) resolution of the area.

the maneuverability and hydrodynamics of the target ship, or the actual magnitude of her rudder during routine sea passage. For this reason, in the following sections CADCAs are presented for the single maneuver of the own ship, while the target remains passive during an approach and only maintains course and speed.

Depending on the final application of CADCA, the area can be presented in different forms. In Fig. 4, the zone depicts MDTCs obtained for various initial headings of the target. To present it in more intuitive way, the values are given for the bearings (BRG_{TS} – outer scale), instead of the headings. Therefore, CADCA can be defined (Equation (4)) as a set of planar positions of the target ship such that, for all bearings MDTC exists and is used to determine the coordinates of the envelope.

2.5. Simulation method

Safety of navigation requires high-accuracy indicators for use in collision avoidance. As presented in Fig. 5, the resolution of CADCA is an important issue with regards to the reliable estimation of a critical maneuvering area. This may result in a massive number of combinations for various operational parameters of ships. Therefore, it was crucial to develop a novel algorithm for efficient determination of CADCA that will provide the possibility to filter out navigational scenarios selected by the user (see Fig. 6). The simulator presented in this paper allows for selecting different numerical ship models and their operational parameters separately for the own ship (OS) and the target ship (TS).

$$CADCA = \left\{(x,y) \in \mathbb{R}^2 | (\forall BRG_{TS} \in \{\alpha \in \mathbb{R} | 0 \le \alpha < 2\pi\})(\exists MDTC \in \{x \in \mathbb{R} | x > 0\})[x = MDTC \cdot \cos(BRG_{TS}) \wedge y = MDTC \cdot \sin(BRG_{TS})]\right\} \quad (4)$$

Where BRG_{TS} means a bearing to the target vessel, *MDTC* stands for the *Minimum Distance to Collision*, x and y are planar coordinates of the MDTC boundary positions.

Configuration files (READ CONFIGS block as per Fig. 6) represent the database which stores information about the models of the ships used. A user can select which vessels will be used for CADCA computation. Important parameters, such as rudder angle or forward speed can be defined there. They enable the simulations to be narrowed further and the results to be filtered. The initial headings and utilized strategies

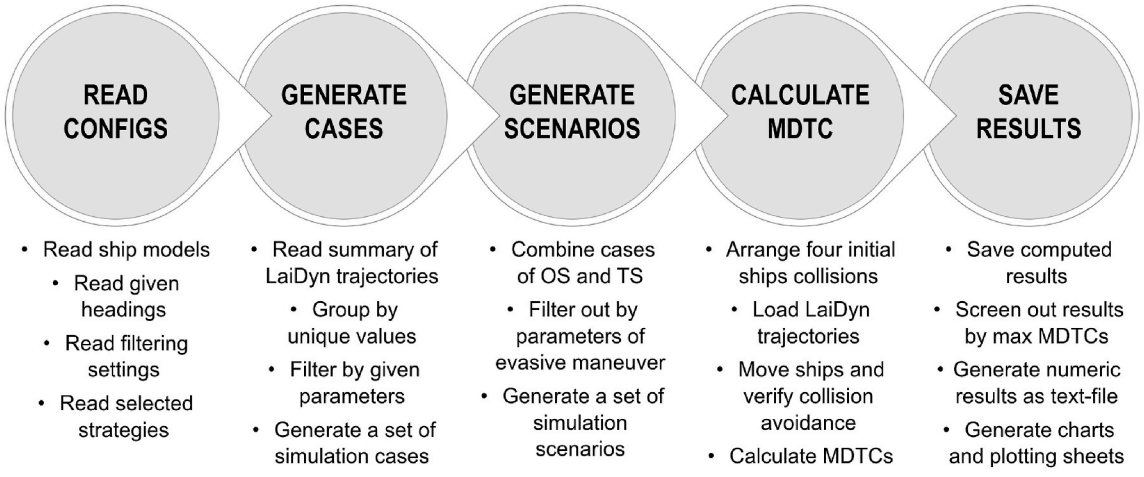

Fig. 6. The general process of operation of the CADCA simulator.

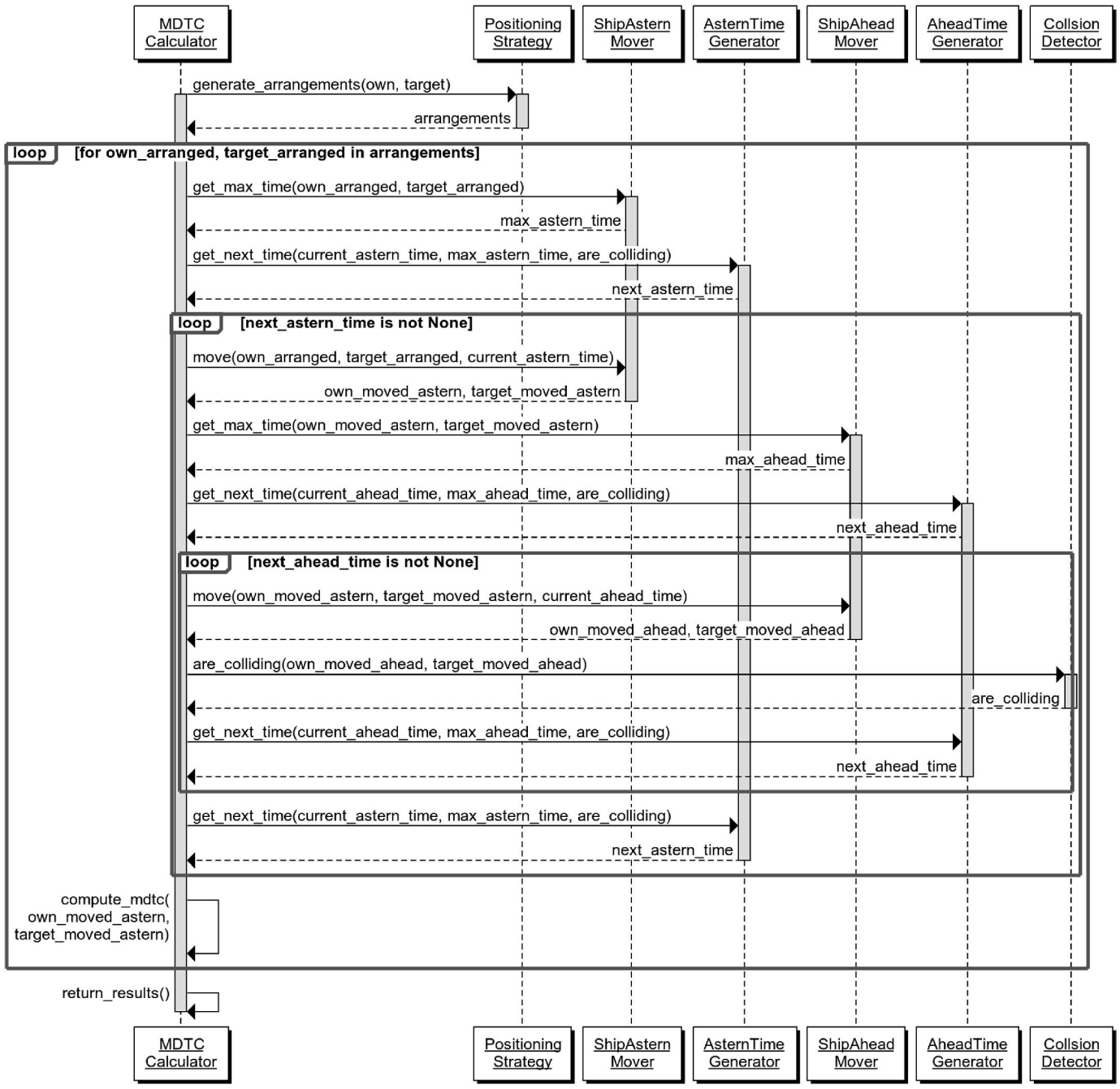

Fig. 7. Sequence diagram presenting the MDTC calculation – part of the CADCA simulator.

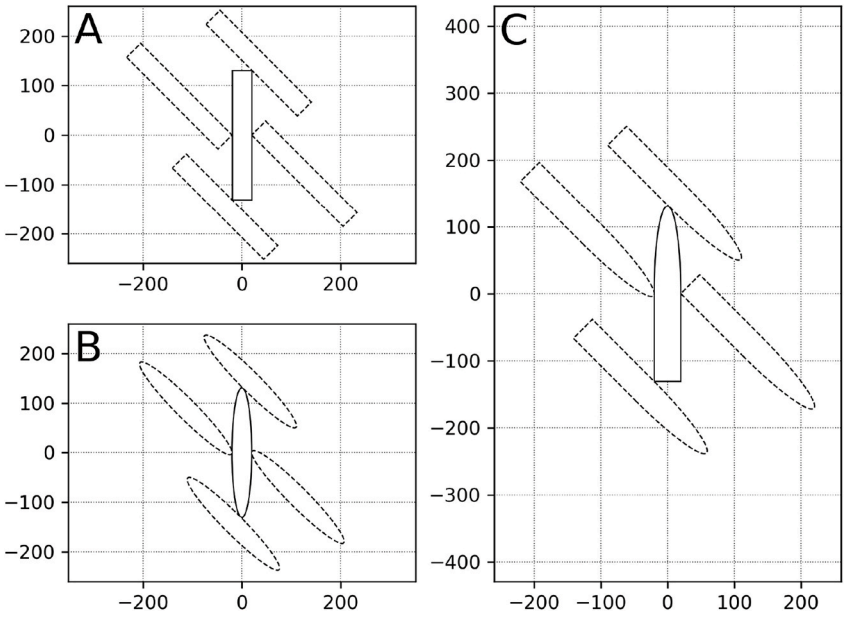

Fig. 8. The initial arrangements of the vessels in four boundary positions for rectangular (A), elliptical (B), and hybrid (C) hulls projections.

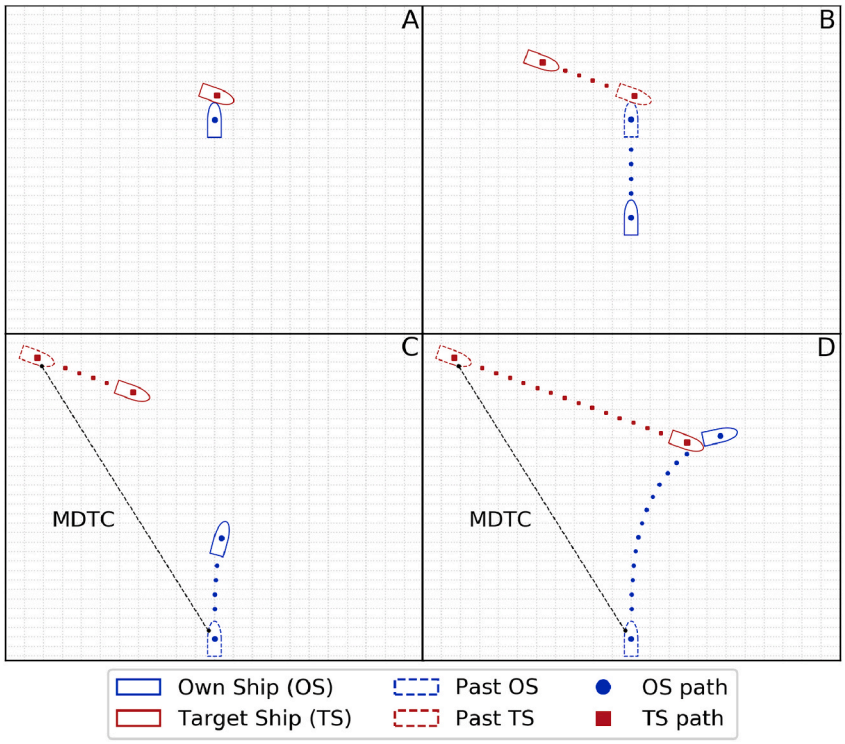

Fig. 9. The sequence of determining MDTC positions. The initial collision of the vessels (A), moving ships astern (B), determination of MDTC position (C), and execution of evasive maneuver (D).

(ships positioning, hulls projections or vessels moving) are then selected.

Consequently, the summary of trajectories delivered by LaiDyn is loaded to determine the *simulation cases*. These may be understood as a set of operating (and if applicable environmental) parameters of ships involved in the encounter. The simulation cases are grouped and filtered according to the user's selection. To begin the computation process, individual OS and TS trajectories are merged into one set. This list is called *simulation scenarios* and contains information about combined cases for both ships with respect to the previous grouping. Final data are passed to the computation stage of the algorithm. The part of the simulator where MDTCs are calculated is the most crucial for the determination of the CADCA introduced. Therefore, it is presented more specifically in the sequence diagram in Fig. 7.

The simulator utilizes a similar approach to the top-down method used in the analysis of maritime accidents. The computer application starts the procedure from the initial collision of two vessels to calculate the MDTC for each encounter. The software generates four boundary positions of the hulls as depicted in Fig. 8. These are represented by tangents to the bow, stern and sides of each ship regarding their headings. It has been assumed that for any given heading, any offset between

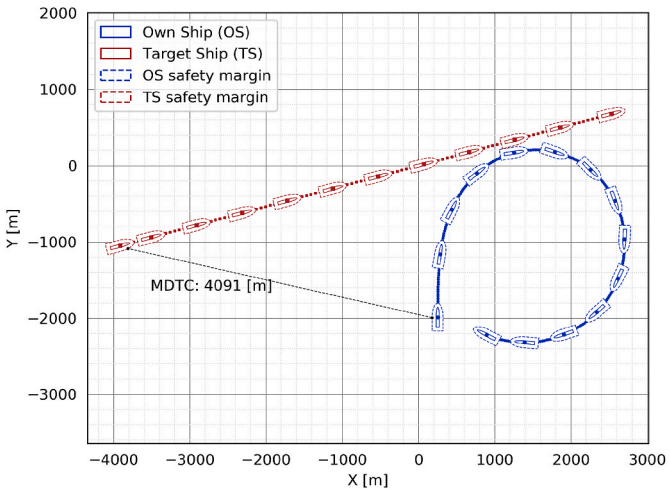

Fig. 10. Plotting sheet of an exemplary scenario with depicted safety margin (dashed line) and ship hull (solid line).

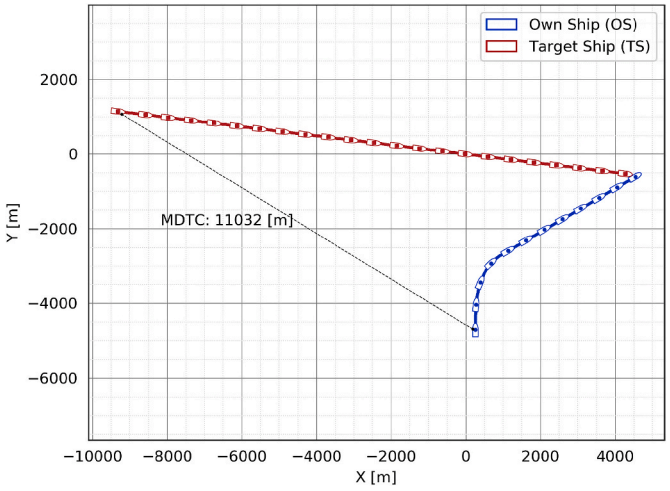

Fig. 11. Example of a navigational scenario when full ship turning circle shall be executed.

the hulls will cause a collision. Therefore, it was sufficient to merely consider the critical positions of the ships instead of all possibilities. As presented in Fig. 8, the simulator allows one of three types of simplified ship's hull shapes to be selected, such as rectangular (A), elliptical (B), and hybrid (C). The results and examples presented in this paper are based on the hybrid type (C), as its shape is the most similar to the real hull of the ship.

From the four boundary ship arrangements (shown in Fig. 8), only the unfavorable one, understood as the simulation result with the largest MDTC, is considered in the CADCA. After the ships' positioning, the sequence of moving astern and ahead is executed as demonstrated in Fig. 9, where the vessels are moved simultaneously backwards and apart for a given time-step. The own ship (OS) proceeds along the trajectory loaded from LaiDyn. In the event of a collision, the algorithm loops for as long as the first chance to avoid an accident occurs. The approach based on simultaneously moving the vessels astern allows an encounter to be reproduced that is compliant with COLREG Rule 7 – *Risk of Collision* assumptions (IMO, 2010).

The method used for CADCA determination faces some limitations mainly related to the accuracy of idealized ship-ship interactions, ship positioning, maneuvering simulations and their associated data intervals. To manage these uncertainties a virtual *safety margin* has been implemented (see dashed lines in Fig. 10). Therefore, the MDTC between safety margins is calculated rather than the hulls of the vessels. The plotting sheet depicting an exemplary simulation scenario with included safety margins is presented (see Fig. 10). All uncertainties identified during the study, which affect the size of introduced safety margin, are further elaborated in detail in Section 4.2.

In navigation practice terms, course alteration is a key part of a vessel's collision avoidance maneuvers. This is because it is more efficient than changing speed, especially for large ships with conventional propulsion and steering devices. According to COLREG Rule 8, the alteration of the course should be large enough to be noticeable and transparent for the second vessel either visually or by radar (IMO, 2010). In this statement, the term *large enough* is rather vague, although in navigational practice it is assumed that an alteration of at least 30° will be executed. Depending on the case, practical recommendations may suggest even larger changes of the course up to 60° or even 90° – e.g. under restricted visibility conditions (Cockcroft and Lameijer, 2012). To keep the alteration of the course large enough and at the same time reasonable, the algorithm introduced in this paper alters the OS's heading by 60°. However, as presented in Fig. 11, the alteration of the course by a fixed value could be inefficient, especially when ships

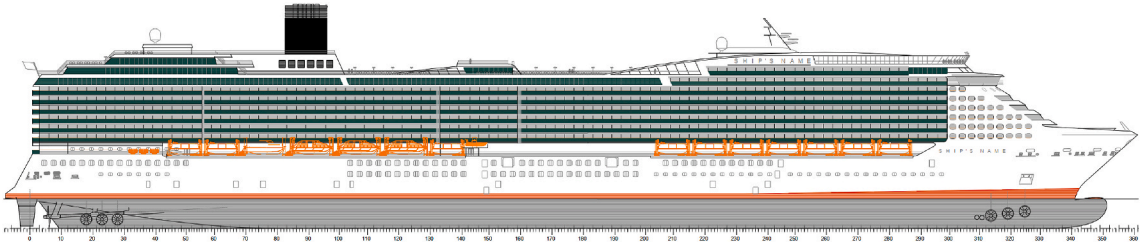

Fig. 12. Floodstand-A (FSA) post-Panamax cruise ship (Kujanpää and Routi, 2009).

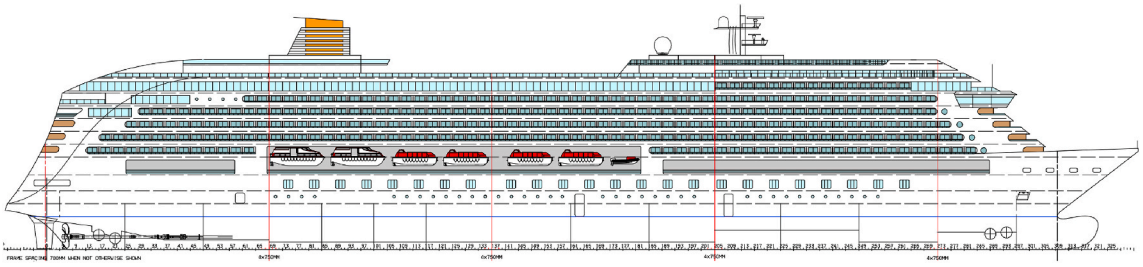

Fig. 13. Floodstand-B (FSB) medium-sized cruise ship (Luhmann, 2009).

proceed at the same speed. In certain cases, the full ship turning circle should be executed instead of a 60° turn, to provide effective evasive action. Such a situation may occur in scenarios where the MDTC value is exceptionally large due to some unfavorable parameters of the encounter, such as mutual headings, same speed of ships, etc. Therefore, to maintain the operational usefulness of the CADCA for onboard applications, the algorithm acts in two ways and suggests a course change of either 60° or 360°.

The results are generated when the overlaying ship trajectory allows for the successful execution of an evasive maneuver. The maximum MDTC value for each simulation scenario is taken into account for further analysis. Finally, computed distances are generated along with radar plots depicting the CADCA. The pseudocode of the described simulator with its generalized mathematical formulation is presented in Algorithm 1.

Algorithm 1. The pseudocode with generalized mathematical formulation of the CADCA simulator.

```
algorithm CalculateMDTC is
    input:    ship ∈ {OS, TS},
              center = (x, y) ∈ ℝ²,
              hull(center, ship) = {(x, y) ∈ ℝ² | (x, y) ∈ projection(ship)},
              scenarios = {S_1, S_2, ..., S_n},
              speed(S_n, ship) ∈ {speed ∈ ℤ | (∃k ∈ ℤ)[speed = 4k] ∧ (12kn ≤ speed ≤ 20kn)},
              heading(S_n, ship) ∈ {α ∈ ℝ | 0 ≤ α < 2π},
              trajectories = {{(x, y) ∈ ℝ²}},
              trajectory(S_n, ship) ∈ trajectories,
              coordinates(S_n, time, ship) ∈ trajectory(S_n, ship)
    output:   MDTC ∈ {x ∈ ℝ | x > 0},
              BRG_TS ∈ {α ∈ ℝ | 0 ≤ α < 2π})

    for each S_n in scenarios do
    OS_center ← (0,0)
    arrangements ← {TS_center ∈ ℝ² | card(hull(TS_center, TS) ∩ hull(OS_center, OS)) = 1}
    for each TS_center in arrangements do
        OS_max_time ← max(card(trajectory(S_n, OS)))
        TS_max_time ← max(card(trajectory(S_n, TS)))
        time_max ← min(OS_max_time, TS_max_time)
            time_astern_start ← 1
            time_astern_end ← time_max
            while (time_astern_start < time_astern_end) do
                time_astern ← (time_astern_start + time_astern_end) / 2
                distance(ship) ← −speed(S_n, ship) · time_astern
                OS_astern_center ← OS_center + (−sin(heading(S_n, OS)) · distance(OS), cos(heading(S_n, OS)) · distance(OS))
                TS_astern_center ← TS_center + (−sin(heading(S_n, TS)) · distance(TS), cos(heading(S_n, TS)) · distance(TS))
                collision ← False
                time_ahead ← 1
                while (scenarios = False) ∧ (time_ahead ≤ time_max) do
                    OS_ahead_center ← OS_astern_center + coordinates(S_n, time_ahead, OS)
                    TS_ahead_center ← TS_astern_center + coordinates(S_n, time_ahead, TS)
                    collision ← (hull(OS_ahead_center, OS) ∩ hull(TS_ahead_center, TS) ≠ ∅)
                    time_ahead ← time_ahead + 1
                end while
                if collision = True then
                    time_astern_start ← time_astern
                else
                    time_astern_end ← time_astern
                end if
            end while
            a ← ((TS_astern_center_y − OS_astern_center_y) / (TS_astern_center_x − OS_astern_center_x))
            b ← OS_astern_center_y − a · OS_astern_center_x
            line ← {(x, y) ∈ ℝ² | y = ax + b}
            OS_closest ← hull(OS_astern_center, OS) ∩ line
            TS_closest ← hull(TS_astern_center, TS) ∩ line
            MDTC(S_n) ← √((TS_closest_x − OS_closest_x)² + (TS_closest_y − OS_closest_y)²)
            BRG_TS(S_n) ← tan⁻¹(a)
        end for
    end for
return MDTC, BRG_TS
```

Table 1
Particulars of the ship models used in the simulation study.

Ship model	Floodstand-A	Floodstand-B
References	Kujanpää and Routi (2009)	Luhmann (2009)
Figure no.	12	13
Length overall, L_{OA} [m]	327.0	238.0
Length between perpendiculars, L_{PP} [m]	300.7	216.8
Beam molded, B [m]	37.4	32.2
Draft design, T_d [m]	8.5	7.2
Draft max., T_{max} [m]	8.8	7.4
Max persons on board	5600	2400
Gross tonnage, GT	125,000	63,000

Table 2
A summary of all the conducted simulations.

Figure no.	14	15	17
OS_{HDG} [°]	000° (North)	000° (North)	000° (North)
OS_{SOG} [kn]	20	12	[12, 20] every 4 kn
$\boldsymbol{OS_{RA}}$ [°]	[5, 35] every 10°	5°	[5, 35] every 5°
$\boldsymbol{OS_{turn}}$	starboard side	starboard side	starboard side
$\boldsymbol{TS_{HDG}}$ [°]	[000, 360) every 1°	[000, 360) every 1°	[000, 360) every 1°
$\boldsymbol{TS_{SOG}}$ [kn]	20	[12, 20] every 4 kn	[12, 20] every 4 kn
$\boldsymbol{TS_{RA}}$ [°]	rudder amidships	rudder amidships	rudder amidships
$\boldsymbol{TS_{turn}}$	keeps her course	keeps her course	keeps her course

3. Results

To investigate whether and how the operating parameters of encountering vessels affect the size and limits of the CADCA, a simulation study was carried out for large (Fig. 12), and medium size passenger vessels (Fig. 13). Both ships are representative of modern cruise ships previously considered in an EU-funded project called *FLOODSTAND: Integrated flooding and standard for stability and crises management* (Kujanpää and Routi, 2009; Luhmann, 2009). In the simulations presented here, these ships were used as OS and TS. Their main particulars are presented in Table 1.

Several data breakdowns have been prepared to investigate how the vessel parameters impact the CADCA in negligible weather conditions. Table 2 outlines a summary of all the conducted simulations. To ensure a high level of accuracy, all CADCAs have been determined for 360 headings of the TS. Thus, for each initial arrangement of the vessels, the OS was always set on a northern course (000°), while the TS heading varies by 1°-step within the range of $TS_{HDG} \in [000°, 360°)$. All figures depicting the CADCA were prepared as polar plots with TS_{BRG} [°] vs. MDTC [NM].

Table 3
Size of the CADCA for a particular rudder angle comparing to the smallest area.

OS_{RA} [°]	Floodstand-A	Floodstand-B
35	100% (ref. value)	100% (ref. value)
25	101%	102%
15	114%	111%
5	188%	178%

3.1. Magnitude of the rudder angle

Simulations of evasive maneuvers using different magnitudes of rudder angle were conducted to investigate how this parameter impacts the CADCA. Scenarios when both vessels proceed at an equal speed of 20 kts are presented in Fig. 14 (FSA on the left, FSB on the right). These were conducted in order to verify the effect of the OS rudder setting. In the simulations, the OS rudder was set to the starboard side at one of four different angles (from 5° to 35° for a 10° step), while the TS maintained her course. In cases where the vessels were on parallel courses, they could not possibly collide. This trivial phenomenon occurred because of negligible external disturbances and the identical speed of both ships. Consequently, these cases were rejected from the analyzed set.

As presented in Fig. 14, the CADCA may vary for different settings of the rudder. However, its change in shape mainly differs significantly for a rudder angle of 5°, while for other angles it is similar. The zones determined for FSA are generally comparable to these obtained for FSB, but with proportionally larger limits. The maximum MDTCs noticed at this stage of the study were around 2.2 NM for Floodstand-A and 1.6 NM for Floodstand-B. For both ships the largest MDTCs were noticed within bearings of 320°–340° when the TS began the simulations with headings within the range of 090°–140°. This means that the worst navigational cases occur in crossing scenarios and in that event the evasive maneuvers should be executed beforehand.

Although the maximum MDTC values for each rudder angle are similar, the sizes of the areas differ. It is necessary to have a maneuvering area almost twice as large for a 5° rudder than for a 35° rudder (1.9 for FSA and 1.8 for FSB). Thus, the smaller rudder angle of the OS, the larger the CADCA. The changes in the required maneuvering area for various rudder settings of both analyzed ships are presented in Table 3.

A significant slip may be observed around the 330° bearing in the vast majority of the simulations. This could happen because of changes in the initial arrangements of the vessels, as depicted in Fig. 8. The algorithm that determines the CADCA selects the opposite set of initial vessel positions as the worst navigation scenario. This issue is elaborated further in Section 4.3, where a method that could be used to reduce the impact of this phenomenon is proposed.

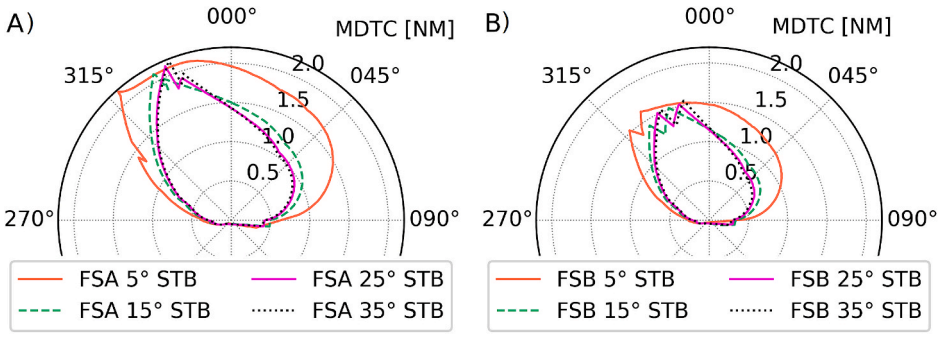

Fig. 14. CADCA for various rudder angles of OS presented for equal speed of the vessels (20 kts). FSA vs. FSA (left) and FSB vs. FSB (right).

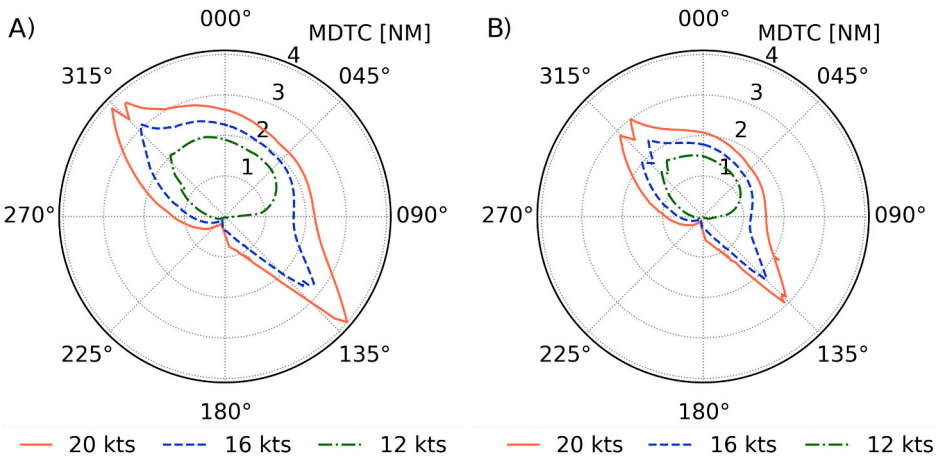

Fig. 15. The CADCA for various initial TS speeds presented for OS rudder angle of starboard 5°. FSA vs. FSA (left) and FSB vs. FSB (right).

3.2. Initial forward speed

The impact of the initial forward speed of the encountering vessels has been verified using a similar approach to the one described in Section 3.1 (see Fig. 15). Accordingly, the rudder angles for both vessels were fixed to investigate solely the effect of the forward speed. The OS rudder was set to starboard 5°, while the TS kept her rudder amidships (Table 2). At the beginning of the simulation, the forward speed of the OS was 12 kts, which is the minimum value considered in the study. The TS speed varied from 12 kts to 16 kts, and eventually increased to 20 kts.

As presented in Fig. 15 and Table 4, the shape and limits of CADCA differ significantly compared to the cases where the rudder angle was investigated. In these scenarios, the OS proceeded at the minimum available speed (12 kts), so the TS is always a threat. Maximum MDTC values were noticed in two sectors of bearings – namely, 120°–135° and 305°–320°. The largest distances for FSA (4.0 and 3.9 NM) were determined, when the target vessel proceeds at maximum speed (20 kts) on courses of 340° (overtaking) and 110° (crossing). This implies that the faster the TS proceeds, the larger the CADCA becomes. The shape of the zone, as well as general findings concerning the values of bearings, courses, and speeds are similar for FSB. The difference between the

Table 4
Size of the CADCA for a particular TS initial speed compared to the smallest area.

TS_{SOG} [kts]	Floodstand-A	Floodstand-B
12	100% (ref. value)	100% (ref. value)
16	231%	224%
20	378%	368%

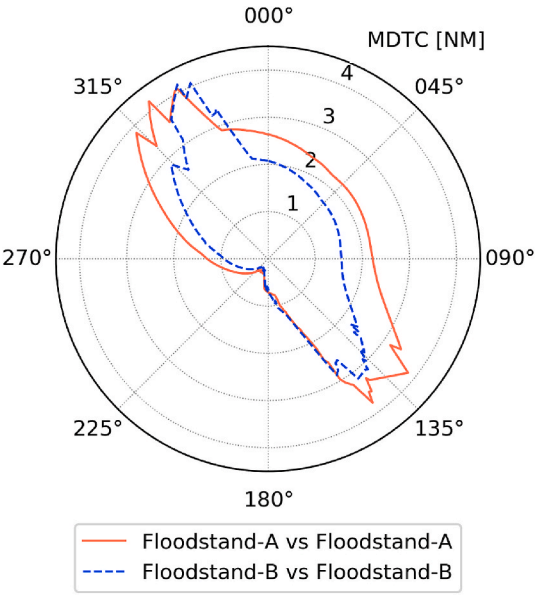

Fig. 17. CADCA for both ships determined for maximal MDTC for all aggregated parameters.

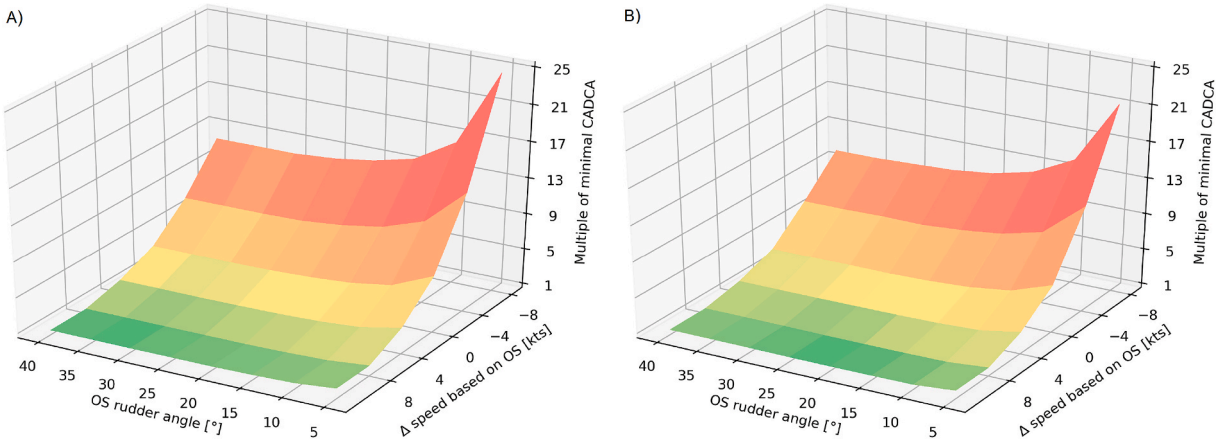

Fig. 16. Comparison of all operational ships parameters and their impact on the CADCA area. FSA vs. FSA (left) and FSB vs. FSB (right).

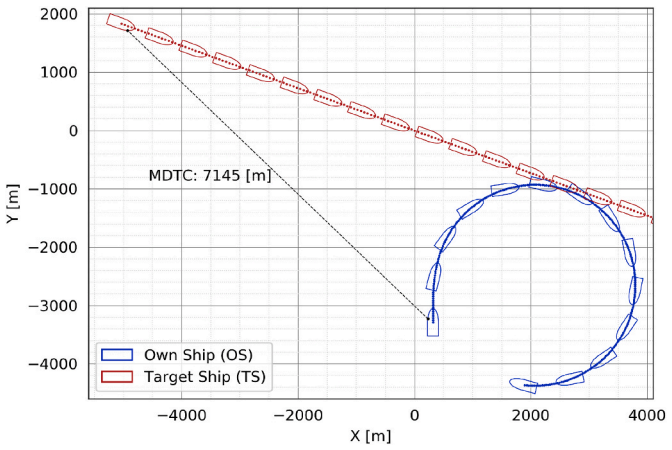

Fig. 18. The sample plotting sheet for a single OS action with the initial heading of the TS at 110°.

CADCA for FSA and FSB is mainly its size, which is proportionally smaller. This is the reason why the maximum observed MDTC for FSB in a comparable case is 3.0 NM.

The appearance of the CADCA abaft of the OS leads to significant changes. Instead of one sector with high MDTCs (as in the previous cases), the second range of large values can be observed on the opposite side (see Fig. 15). Thus, when the TS starts the simulation with an initial heading of around 340° at 20 kts, it leads to the maximum distance being generated astern of the OS. The presence of two dangerous sectors arises from the unfavorable speed difference between the vessels and this causes a significant increase in the required maneuvering area. Because the TS proceeds faster than the OS, she is always a threat. The relative speed seems to be of crucial significance in the analyzed cases. This could be confirmed by the shape of the zone for $TS_{SOG} = 12$ kts, when the encountering ships are equally fast and the CADCA has no additional sector abaft. The second reason for the additional dangerous sector is the direction of the ship's turn. Assuming that the OS executed a turn to the starboard side, the TS may overtake her in the vast majority of analyzed scenarios. Such a situation would lead to maneuvering toward the TS. Therefore, if the observed TS is faster than the OS, especially keen monitoring is required not only on forward of the beam, but also abaft, and particularly on the side where the evasive maneuver will be executed (most frequently the starboard side).

3.3. Comparative analysis

In order to compare how the operational parameters of encountering vessels may affect the CADCA, aggregated results were prepared for both ship models. To this end, simulations of all remaining cases, which are not only limited to the combinations shown in Table 2 were conducted. Then, all the determined areas were compared and color-coded depending on their impact on the size of the area, as shown in Fig. 16. The CADCA for FSA and FSB obtained for maximal MDTC values, when all possible parameter combinations are aggregated, is presented in Fig. 17.

The surface plots prepared to compare the CADCA sizes indicate that the size of the required maneuvering area may also depend on the

Table 5
Summary of MDTC results in the analyzed case of a single LMM, for the example $TS_{HDG} = 110°$.

	TS_{RA} [°]	0 (rudder amidships)			
OS_{RA} [°]	TS_{SOG} [kts] / OS_{SOG} [kts]	12	16	20	Maximum MDTC [NM]
		MDTC [m]			
5 (STB)	12	3705	5116	7145	3.86
	16	2992	3784	4865	2.63
	20	2662	3197	3863	2.09
10 (STB)	12	3208	4314	5315	2.87
	16	2530	3307	4128	2.23
	20	2243	2760	3410	1.84
15 (STB)	12	2893	3795	4617	2.49
	16	2309	2960	3644	1.97
	20	2054	2495	3057	1.65
20 (STB)	12	2718	3525	4247	2.29
	16	2174	2782	3407	1.84
	20	1939	2316	2865	1.55
25 (STB)	12	2621	3383	4050	2.19
	16	2075	2686	3270	1.77
	20	1873	2271	2764	1.49
30 (STB)	12	2578	3312	3944	2.13
	16	2032	2645	3206	1.73
	20	1832	2253	2723	1.47
35 (STB)	12	2584	3312	3935	2.12
	16	2039	2645	3206	1.73
	20	1832	2253	2724	1.47
Maximum MDTC [NM]		2.00	2.76	3.86	**3.86**

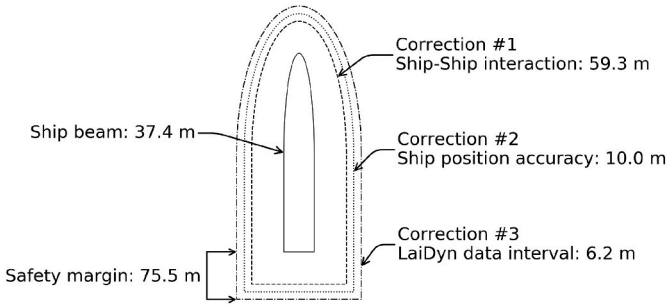

Fig. 19. Components of the safety margin and values of applied corrections for Floodstand-A at 20 kts.

operating parameters of the vessels. Visualizations of these charts confirm that the relationship between the rudder angle and relative speed is similar for both analyzed ship models. However, when comparing areas to the smallest determined CADCA, it can be noticed that the size of the area may increase multiple times depending on the combination of parameters. For example, in the most unfavorable conditions, the CADCA is even 24.6 times larger for FSA and 21.3 times for FSB. The conducted analysis indicates that the smaller the OS rudder angle and the faster the TS, the larger the CADCA.

As part of a more detailed analysis of the MDTC values under CADCA, one initial heading of the TS ($TS_{HDG} = 110°$) was selected for crossing scenario. Ships trajectories for the most unfavorable combination of operational parameters (i.e. lowest rudder angle and OS speed) are depicted in Fig. 18. Detailed results of computed MDTCs are given in Table 5. The tabular data have been color-coded, with green indices for the lowest MDTC and red the highest MDTC. As presented, the relation between calculated distance and operating parameters of the vessels is evident. Also, along with the increase of the speed difference between encountering ships, the MDTC value rises. The analysis of computed values re-confirms the trend that when the rudder angle increases, the distance between the ships decreases.

The maximum MDTC noticed when the TS proceeds with a heading of 110° equals 3.9 NM. The opposite situation leads to the most advantageous scenario when the value of MDTC is the lowest, and the maneuver can be executed at the latest moment. When the OS proceeds at the maximum speed and she sets the rudder at 35° to starboard, the computed MDTC for the analyzed case is 1 NM. Therefore, for the selected TS heading (110°), the MDTC is almost four times lower in the best case than in the worst scenario.

4. Discussion

The results of the study confirm that during evasive maneuver planning, ship dynamics should be taken into account. The introduced *Collision Avoidance Dynamic Critical Area* (CADCA) seems to be a valuable indicator for enhancing maritime safety. Thus, the concept presented could be useful within the context of broader applications of practical relevance to maritime safety. CADCA could be implemented as a component of i) existing navigational equipment (e.g. overlay in the ARPA) ii) onboard Decision Support System (DSS), iii) collision-avoidance algorithms for MASS, iv) traffic monitoring and risk assessment tools. Notwithstanding, the currently proposed method and the study cases presented face some limitations and may be prone to certain uncertainties as explained below.

4.1. Limitations

Limitations and uncertainties identified relate to the minimum consideration of negligible environmental disturbances included in the CADCA and the utilization of one software for delivering input files with the ship dynamics modeled. Essentially, the aspect of COLREGs in the CADCA is not a limitation and arises from the assumptions of the presented concept.

Hydrometeorological factors – mainly wind and waves – should be taken into account in the CADCA to reflect real operational conditions. The impact of weather could be considered with a more complex approach than a mere observation of vessel drift in trajectory delivered by LaiDyn. It is especially worth considering that preliminary research confirms that a 6DoF motion model can be used to verify environmental impact on ship behavior (Gil et al., 2019a). Excessive values of translational and rotational motions could be detected during an evasive maneuver. Therefore, this may result in the consideration of loading condition or ship stability in a close-quarters situation. Further investigations on how these parameters affect the CADCA limits would be valuable for the development of the presented indicator (Gil et al., 2019a).

With regards to COLREGs, the proposed method of CADCA determination seems to be sufficient, although these two issues should be explicitly separated. Even though this approach is directly linked to COLREG Rule 17 (incl. action taken by the stand-on vessel), the algorithm computes parameters for many initial target headings. Therefore, the indicator is not directly related to the COLREG Rules 13–15, which are used to regulate the conduct of vessels involved in an encounter depending on their mutual arrangement. The envelope is calculated

Table 6
Uncertainties identified in the study with applied corrections for Floodstand-A at full sea speed.

Uncertainty	Description	Method of handling	Correction
Hull interaction	During the passing and overtaking of two vessels, forces between their hulls occur (Lee, 2015; PIANC, 2014; Vantorre et al., 2002; Yuan et al., 2015). This phenomenon can lead to ship contact if there is no sufficient clearance between them. Thus, it should be considered during the CADCA determination.	The correction based on (PIANC, 2014) ship-ship interaction coefficient for a similar type of the vessel is applied. After adjusting the overtaking factor accordingly to the ship beam, it is used as a component of the safety margin.	59.3 m
Position accuracy	The position of the ship during real operation is obtained by the GNSS with limited accuracy. The offset in vessel position could cause erroneous calculation of the MDTC. Thus, the position error should be considered in the process of the CADCA computation to provide reliable results.	Because of position accuracy of the GNSS, the correction based on minimum requirements of (IMO, 2011) is applied as a component of the safety margin.	10.0 m
LaiDyn model	The usage of the LaiDyn model can lead to inaccurate representation of the ship's motions and her maneuvering. However, the software has been used in several studies and validated in a few tests. During towing tank and benchmark examinations (ITTC, 2005, 2002; Matusiak and Stigler, 2012), the results of LaiDyn validation have been recognized as reliable. Thus, additional corrections are not required.	Not applicable. In further works, various models could be used to compare the results delivered by LaiDyn.	n/a
Data interval	Ship trajectories are generated in LaiDyn software for a given time-step. The data interval used in the study equals 0.6 s. The frequency of ship coordinates impacts the precision of the MDTC determination. Thus, the distance covered by the ship proceeding at a given speed should be included in the CADCA computation process.	The correction based on an initial simulation speed for a given data interval (0.6 s) is applied as a component of the safety margin.	6.2 m

regardless of the regulations, while its shape is based solely on hydrodynamics and ship maneuvering. Bearing in mind that the CADCA may be determined in situations that may assume compliance with the COLREGs or not, it is crucial to always take the utmost precaution. Therefore, to avoid misinterpretations, nautical background and seagoing experience should not be underestimated.

4.2. Dealing with uncertainties

The uncertainties identified in CADCA involve the interaction between ships hulls, the accuracy of the vessels' positions, the utilization of LaiDyn model, and the interval of the data therein. To reflect the effect of uncertainties on the CADCA, a virtual safety margin is introduced. The example dedicated to large passenger ship Floodstand-A at a forward speed of 20 kts is depicted in Fig. 19 and described in Table 6.

Ship-ship interaction is a phenomenon that results from hydrodynamic forces acting between the hulls. When two vessels proceed alongside each other, it is necessary to maintain a relevant passing distance to avoid a collision. Therefore, it was necessary to include the required clearance between the vessels in the process of CADCA determination. Hull interactions may differ depending on the type of encounter (Vantorre et al., 2002), the difference in vessel dimensions (Yuan et al., 2015), as well as their speeds (Mousaviraad et al., 2016). The required distance between two ships is larger for overtaking than for passing (Lee, 2015; PIANC, 2014) maneuvers. Therefore, in this study the overtaking scenario was selected to assume the worst case. The empirical coefficient provided by the *World Association for Waterborne Transport Infrastructure* (PIANC, 2014) was applied in the conducted study. This correction factor was selected for the most similar type of the vessel and adjusted to sizes of the ship models used.

The IMO requirements for radio-navigational systems divide position accuracy into open sea and areas in the vicinity of the shoreline (IMO, 2011). For ocean waters, the position error should be not greater than 100 m, while in coastal waters and harbor approaches it should not exceed 10 m (IMO, 2011). However, due to the development of supporting systems for ship positioning, the expected accuracy is even higher, also in a dynamic maritime environment (Specht et al., 2019). Therefore, the maximum acceptable value of the position error (10 m) was applied as a component of the safety margin.

Finally, the data interval of ship trajectories delivered by LaiDyn was 0.6 s. For this particular time-step, the distance covered by the ship at a given speed was applied in the safety margin by enlarging it. In further studies, the data frequency could be increased as much as the LaiDyn software or other program allows.

4.3. Future work

Further research related to the CADCA concept should be focused on two major tasks: i) reflecting the real operational conditions of the ship; ii) increasing the accuracy and efficiency of the area determination. A better simulation of a vessel's operational conditions could be achieved, for instance, by considering the presence of environmental disturbances. Including the impact of wind and waves would appear to be crucial in order to verify how weather affects CADCA limits. Because LaiDyn software can simulate vessel behavior in various hydrometeorological conditions, development of the algorithm presented in Section 2.5 could be proposed in further research.

Additionally, in the examination of the initial vessel speed conducted, only the TS velocity changed, while the OS maintained the same speed in each simulation. As *the rudder effect* coupling the rudder angle and the ship's speed does exist, this part of the study should be thoroughly investigated in further works. An increase in ship speed during maneuver execution (e.g. turning circle) causes an increase in the lift force acting on the deflected rudder, and so the tactical diameter is expected to be affected. This relationship could be observed and analyzed in future work by verifying various OS speeds for the same rudder angle used during a variety of evasive maneuver scenarios.

The accuracy of CADCA could be refined by improving the numerical and operational inadequacies implemented in the model. For example, it is believed that the sharp slip observed in the area could be reduced by changing the method of initial ship positioning. This might be achieved by increasing the amount of initial positioning of the ships involved in an encounter scenario. Their number should be linked with the safety margin dimensions in order to provide relevant coverage and maintain CADCA shape consistency. The safety margin could be dynamic and adjust its dimensions in each simulation to reduce any overestimation. The correction resulting from ship-ship interaction should vary depending on the type of an encounter. Taking into account the angles between the heading lines of the ships could improve assumptions and provide different clearances during passing and/or overtaking scenarios.

The use of more ship models and their loading conditions for testing and validating the CADCA concept could allow for more conclusive comparisons in terms of CADCA size and limits for various types of vessels. The implementation of maneuvering trajectories that are reliable using a faster and more practical maneuvering simulator (Taimuri et al., 2019) could reduce the uncertainties caused by the current usage of a single maneuvering program.

It is believed that all improvements aimed at producing a better simulation of reality could result in the future implementation of the CADCA as an indicator for onboard DSS. In such a situation, the particulars of the TS and her speed would be obtained from existing navigational equipment like the AIS (*Automatic Identification System*). Then, approximated ship behavior for these parameters could be sourced from the meta-model built using BNN (*Bayesian Belief Networks*) for a group of representative ships. The use of such a tool could deliver critical maneuvering areas, that may change their limits and shapes dynamically in real-time.

5. Conclusions

This paper had three main objectives. The first was to present a novel indicator used in an encounter between two vessels under negligible environmental disturbances. The *Collision Avoidance Dynamic Critical Area* (CADCA) was introduced in a version for onboard DSS. The area surrounds the own ship and changes its limits for various operating parameters of the vessels. The results suggest that the introduced zone could be useful for OOWs in the determination of the critical maneuvering area, as well as for planning evasive action. It is worth noting that cases where the target ship maintains her course and speed are essential for the navigational safety, due to the larger area required. Additionally, in these scenarios knowledge about the maneuvering and hydrodynamics of the target is not necessarily required. Future work on this concept could result in the development of a fully dynamic version of the CADCA, which adjusts its limits in real-time using data from navigational equipment. However, this could be used not only as a part of the onboard DSS. Another potential application of the CADCA is to create a collision-avoidance algorithm for MASS. The introduced zone could be also used in maritime traffic monitoring and risk assessment as a near-miss criterion.

The second aim of the study was to introduce an algorithm to efficiently determine the CADCA. The principles of its operation were elaborated along with a description of the MDCT calculation process. The method of ship positioning in the simulator was presented using four boundary arrangements. However, this could be improved in order to eliminate identified limitation, namely the sharp slip observed in the CADCA. In future work, the software should be also developed to include the remaining operational parameters of the vessels and to consider environmental conditions.

The third objective was to investigate the impact of the rudder setting initial forward speed for a single evasive action of the own ship. The results of the simulations conducted confirmed that the CADCA varies in size for different operating parameters of encountering ships.

Thus, its dynamics should be considered while planning an evasive maneuver. For various magnitudes of rudder angles when the vessels proceed at the same speed, the danger zone is located ahead of the beam. However, for different speeds of the TS, the CADCA has two sectors of large MDTC values. Therefore, in some navigational scenarios, the sector abaft the beam should be likewise considered as a potential threat. In certain cases when the own ship sets the rudder to the smallest available angle (5°) and proceeds slower than the target, it leads to the worst navigational scenario when the largest maneuvering area is required.

Declaration of competing interest

The authors declare that they have no known competing financial interests or personal relationships that could have appeared to influence the work reported in this paper.

CRediT authorship contribution statement

Mateusz Gil: Conceptualization, Methodology, Software, Validation, Formal analysis, Investigation, Data curation, Writing - original draft, Writing - review & editing, Visualization. **Jakub Montewka:** Conceptualization, Methodology, Writing - review & editing, Supervision. **Przemyslaw Krata:** Conceptualization, Formal analysis, Writing - review & editing. **Tomasz Hinz:** Resources, Data curation. **Spyros Hirdaris:** Writing - review & editing, Supervision, Project administration, Funding acquisition.

Acknowledgments

The research presented in the paper was conducted under EU Horizon 2020 project FLooding Accident REsponse (FLARE – Contract No. 814753). Przemyslaw Krata appreciated financial support of the grant WN/2020/PZ/02 funded by the Faculty of Navigation, Gdynia Maritime University for writing - review & editing.

References

Acanfora, M., Krata, P., Montewka, J., Kujala, P., 2018. Towards a method for detecting large roll motions suitable for oceangoing ships. Appl. Ocean Res. 79, 49–61. https://doi.org/10.1016/j.apor.2018.07.005.

Acanfora, M., Montewka, J., Hinz, T., Matusiak, J., 2017. Towards realistic estimation of ship excessive motions in heavy weather. A case study of a containership in the Pacific Ocean. Ocean. Eng. 138, 140–150. https://doi.org/10.1016/j.oceaneng.2017.04.025.

Baldauf, M., Benedict, K., Krúger, C., 2014. Potentials of e-navigation – enhanced support for collision avoidance. TransNav, the International Journal on Marine Navigation and Safety of Sea Transportation 8, 613–617. https://doi.org/10.12716/1001.08.04.18.

Baldauf, M., Hong, S.-B., 2016. Improving and assessing the impact of e-navigation applications. International Journal of e-Navigation and Maritime Economy 4, 1–12. https://doi.org/10.1016/j.enavi.2016.06.001.

Bole, A.G., Wall, A., Norris, A., 2014. Radar and ARPA Manual: Radar, AIS and Target Tracking for Marine Radar Users, third ed. Butterworth-Heinemann, Oxford.

Chen, P., Huang, Y., Mou, J., van Gelder, P.H.A.J.M., 2019. Probabilistic risk analysis for ship-ship collision: state-of-the-art. Saf. Sci. 117, 108–122. https://doi.org/10.1016/j.ssci.2019.04.014.

Chen, P., Huang, Y., Mou, J., van Gelder, P.H.A.J.M., 2018. Ship collision candidate detection method: a velocity obstacle approach. Ocean. Eng. 170, 186–198. https://doi.org/10.1016/j.oceaneng.2018.10.023.

Cockcroft, A.N., Lameijer, J.N.F., 2012. Guide to the Collision Avoidance Rules - International Regulations for Preventing Collisions at Sea, seventh ed.

Colley, B.A., Curtis, R.G., Stockel, C.T., 1983. Manoeuvring times, domains and arenas. J. Navig. 36, 324–328. https://doi.org/10.1017/S0373463300025030.

Crosbie, J.W., 2008. Manoeuvring in the agony of the moment. J. Navig. 61, 734–738. https://doi.org/10.1017/S0373463308004852.

Cummins, W.E., 1962. The Impulse Response Function and Ship Motions (Hydromechanics Laboratory Research and Development Report No. 1661). Department of The Navy David Taylor Model Basin.

EMSA, 2018. Annual Overview of Marine Casualties and Incidents 2018. EMSA - European Maritime Safety Agency, Lisboa.

Gil, M., Montewka, J., Krata, P., Hinz, T., 2019a. Ship stability-related effects on a critical distance of collision evasive action. In: Proceedings of the 17th International Ship Stability Workshop. Presented at the 17th International Ship Stability Workshop, Helsinki, Finland, pp. 231–238.

Gil, M., Montewka, J., Krata, P., Hinz, T., Hirdaris, S., 2020a. Semi-dynamic ship domain in the encounter situation of two vessels. In: Soares, C.G. (Ed.), Developments in the Collision and Grounding of Ships and Offshore Structures. Taylor and Francis Group, London, pp. 301–307.

Gil, M., Wróbel, K., Montewka, J., 2019b. Toward a method evaluating control actions in STPA-based model of ship-ship collision avoidance process. J. Offshore Mech. Arctic Eng. 141, 051105 https://doi.org/10.1115/1.4042387.

Gil, M., Wróbel, K., Montewka, J., Goerlandt, F., 2020b. A bibliometric analysis and systematic review of shipboard Decision Support Systems for accident prevention. Saf. Sci. 128, 104717. https://doi.org/10.1016/j.ssci.2020.104717.

Hilgert, H., 1983. Defining the close-quarters situation at Sea. J. Navig. 36, 454–461. https://doi.org/10.1017/S0373463300039801.

Hinz, T., Acanfora, M., Montewka, J., Krata, P., Matusiak, J.E., 2018. Meta-model assessing the probability of exceeding the allowed acceleration limits, with the use of bayesian network. In: Presented at the 13th International Conference on the Stability of Ships and Ocean Vehicles, Kobe, Japan.

IMO, 2014. SOLAS : International Convention for the Safety of Life at Sea, 1974, as Amended 2014, Consolidated Edition. IMO Publishing, London. 2014.

IMO, 2011. Resolution A.1046(27) : WORLDWIDE RADIONAVIGATION SYSTEM.

IMO, 2010. COLREG : Convention on the International Regulations for Preventing Collisions at Sea, 1972, Consolidated Edition. International Maritime Organization, London. 2003.

IMO, 2008. MSC 85/26/Add.1 - Annex 20 - Strategy for the Development and Implementation of E-Navigation.

ITTC, 2005. Final report and recommendations to the 24th ITTC. In: Presented at the 24rd International Towing Tank Conference, pp. 369–408.

ITTC, 2002. The specialist committee on prediction of extreme ship motions and capsizing final report and recommendations to the 23rd ITTC. In: Presented at the 23rd International Towing Tank Conference, pp. 619–748.

Journée, J.M.J., Massie, W.W., 2001. OFFSHORE HYDROMECHANICS, first ed. ed. Delft University of Technology, Delft.

Koszelew, J., Wołejsza, P., 2017. Determination of the last moment manoeuvre for collision avoidance using standards for ships manoeuvrability. Annu. Navig. 24, 301–313. https://doi.org/10.1515/aon-2017-0022.

Krata, P., Montewka, J., Hinz, T., 2016. Towards the assessment of critical area in a collision encounter accounting for stability conditions of a ship. Prace Naukowe Politechniki Warszawskiej. Transport 114, 169–178.

Krata, P., Szlapczynska, J., 2018. Ship weather routing optimization with dynamic constraints based on reliable synchronous roll prediction. Ocean. Eng. 150, 124–137. https://doi.org/10.1016/j.oceaneng.2017.12.049.

Kujanpää, J., Routi, A.-L., 2009. Concept Ship Design A (Deliverable D1.1a No. FP7-RTD-218532), FLOODSTAND : Integrated Flooding and Standard for Stability and Crises Management. STX Europe.

Kukkanen, T., 1995. Sealoads Versio 6.0 - Ohjelman Käyttöohje (No. VTT VAL42034). VTT VALMISTUSTEKNIIKKA, Espoo.

Lee, S., 2015. A numerical study on ship-ship interaction in shallow and restricted waterway. International Journal of Naval Architecture and Ocean Engineering 7, 920–938. https://doi.org/10.1515/ijnaoe-2015-0064.

Lenart, A.S., 2015. Analysis of collision threat parameters and criteria. J. Navig. 68, 887–896. https://doi.org/10.1017/S0373463315000223.

Lenart, A.S., 1983. Collision threat parameters for a new radar Display and plot technique. J. Navig. 36, 404–410. https://doi.org/10.1017/S0373463300039758.

Luhmann, H., 2009. Concept Ship Design B (Deliverable D1.1b No. FP7- RTD-218532), FLOODSTAND : Integrated Flooding and Standard for Stability and Crises Management. MEYER WERFT GmbH.

Ma, F., Wu, Q., Yan, X., Chu, X., Zhang, D., 2015. Classification of automatic radar plotting Aid targets based on improved fuzzy C-means. Transport. Res. C Emerg. Technol. 51, 180–195. https://doi.org/10.1016/j.trc.2014.12.001.

Manderbacka, T., Matusiak, J., Ruponen, P., 2011. Ship motions caused by time-varying extra mass on board. In: Proceedings of the 12th International Ship Stability Workshop, pp. 263–270.

Matusiak, J., 2017. Dynamics of a Rigid Ship. Aalto University publication series SCIENCE + TECHNOLOGY, 2/2017. Aalto University.

Matusiak, J., 2007. On certain types of ship responses disclosed by the two-stage approach to ship dynamics. Archives of Civil and Mechanical Engineering 7, 151–166. https://doi.org/10.1016/S1644-9665(12)60233-7.

Matusiak, J., Stigler, C., 2012. Ship motion in irregular waves during a turning circle manoeuvre. In: Spyrou, K.J., T, N. (Eds.), The 11TH International Conference on the Stability of Ships and OCEAN Vehicles. National Technical University of Athens, School of Naval Architecture and Marine Engineering, Athens, pp. 291–298, 23-28 September 2012.

Matusiak, J.E., 2011. On the non-linearities of ship's restoring and the Froude-Krylov wave load part. International Journal of Naval Architecture and Ocean Engineering 3, 111–115. https://doi.org/10.2478/IJNAOE-2013-0052.

Miloh, T., 1975. Determination of Critical Maneuvers for Collision Avoidance Using the Theory of Differential Games. Technische Universität Hamburg-Harburg, Hamburg.

Montewka, J., Goerlandt, F., Kujala, P., 2012. Determination of collision criteria and causation factors appropriate to a model for estimating the probability of maritime accidents. Ocean. Eng. 40, 50–61. https://doi.org/10.1016/j.oceaneng.2011.12.006.

Montewka, J., Goerlandt, F., Kujala, P., 2011a. A new definition of a collision zone for a geometrical model for ship-ship collision probability estimation. In: Methods and Algorithms in Navigation. CRC Press, pp. 93–100. https://doi.org/10.1201/b11344-16.

Montewka, J., Goerlandt, F., Lammi, H., Kujala, P., 2011b. A method for assessing a causation factor for a geometrical MDTC model for ship-ship collision probability

estimation. In: Methods and Algorithms in Navigation. CRC Press, pp. 65–73. https://doi.org/10.1201/b11344-13.
Montewka, J., Hinz, T., Kujala, P., Matusiak, J., 2010. Probability modelling of vessel collisions. Reliab. Eng. Syst. Saf. 95, 573–589. https://doi.org/10.1016/j.ress.2010.01.009.
Montewka, J., Krata, P., 2014. Towards the assessment of a critical distance between two encountering ships in open waters. European Journal of Navigation 12, 7–14.
Mousaviraad, S.M., Sadat-Hosseini, S.H., Stern, F., 2016. Ship–ship interactions in calm water and waves. Part 1: analysis of the experimental data. Ocean. Eng. 111, 615–626. https://doi.org/10.1016/j.oceaneng.2015.10.035.
Ni, S., Liu, Z., Cai, Y., 2019. Ship manoeuvrability-based simulation for ship navigation in collision situations. J. Mar. Sci. Eng. 7, 90. https://doi.org/10.3390/jmse7040090.
Ożoga, B., Montewka, J., 2018. Towards a decision support system for maritime navigation on heavily trafficked basins. Ocean. Eng. 159, 88–97. https://doi.org/10.1016/j.oceaneng.2018.03.073.
Perera, L.P., Carvalho, J.P., Guedes Soares, C., 2012. Intelligent ocean navigation and fuzzy-bayesian decision/action formulation. IEEE J. Ocean. Eng. 37, 204–219. https://doi.org/10.1109/JOE.2012.2184949.
Perera, L.P., Ferrari, V., Santos, F.P., Hinostroza, M.A., Guedes Soares, C., 2015. Experimental evaluations on ship autonomous navigation and collision avoidance by intelligent guidance. IEEE J. Ocean. Eng. 40, 374–387. https://doi.org/10.1109/JOE.2014.2304793.
PIANC, 2014. MarCom WG 121: Harbour Approach Channels - Design Guidelines.
Riggs, R.F., 1975. A modern collision avoidance Display technique. J. Navig. 28, 143–155. https://doi.org/10.1017/S0373463300037681.
Riggs, R.F., O'Sullivan, J.P., 1980. An analysis of the point of possible collision. J. Navig. 33, 259–283. https://doi.org/10.1017/S037346330003527X.
Rymarz, W., 2007. The determination of a minimum critical distance for avoiding action by a stand-on vessel as permitted by Rule 17a) ii). TransNav, the International Journal on Marine Navigation and Safety of Sea Transportation 1, 63–68.
Smierzchalski, R., 2005. Ships' domains as collision risk at sea in the evolutionary method of trajectory planning. In: Saeed, K., Pejaś, J. (Eds.), Information Processing and Security Systems. Springer US, pp. 411–422.
Smierzchalski, R., Michalewicz, Z., 2000. Modeling of ship trajectory in collision situations by an evolutionary algorithm. IEEE Trans. Evol. Comput. 4, 227–241. https://doi.org/10.1109/4235.873234.
Specht, C., Pawelski, J., Smolarek, L., Specht, M., Dabrowski, P., 2019. Assessment of the positioning accuracy of DGPS and EGNOS systems in the bay of gdansk using maritime dynamic measurements. J. Navig. 72, 575–587. https://doi.org/10.1017/S0373463318000838.
Sweeney, J., 1992. Starboard hand Rule under the 1972 collision regulations. J. Marit. Law Commer. 23, 19.
Szlapczynska, J., Szlapczynski, R., 2017. Heuristic method of safe manoeuvre selection based on collision threat parameters areas. TransNav, the International Journal on Marine Navigation and Safety of Sea Transportation 11, 591–596. https://doi.org/10.12716/1001.11.04.03.
Szlapczynski, R., 2008. Fuzzy collision threat parameters area (FCTPA) – a new Display proposal. TransNav, the International Journal on Marine Navigation and Safety of Sea Transportation 2, 4.
Szlapczynski, R., Krata, P., 2018. Determining and visualizing safe motion parameters of a ship navigating in severe weather conditions. Ocean. Eng. 158, 263–274. https://doi.org/10.1016/j.oceaneng.2018.03.092.
Szlapczynski, R., Krata, P., Szlapczynska, J., 2018a. Ship domain applied to determining distances for collision avoidance manoeuvres in give-way situations. Ocean. Eng. 165, 43–54. https://doi.org/10.1016/j.oceaneng.2018.07.041.
Szlapczynski, R., Krata, P., Szlapczynska, J., 2018b. A ship domain-based method of determining action distances for evasive manoeuvres in stand-on situations. J. Adv. Transport. 2018, 1–19. https://doi.org/10.1155/2018/3984962.
Szlapczynski, R., Smierzchalski, R., 2009. Supporting navigator's decisions by visualizing ship collision risk. Pol. Marit. Res. 16, 83–88. https://doi.org/10.2478/v10012-008-0015-7.
Szlapczynski, R., Szlapczynska, J., 2017. A method of determining and visualizing safe motion parameters of a ship navigating in restricted waters. Ocean. Eng. 129, 363–373. https://doi.org/10.1016/j.oceaneng.2016.11.044.
Taimuri, G., Mikkola, T., Matusiak, J., Kujala, P., Hirdaris, S., 2019. The influence of hydrodynamic assumptions on ship maneuvering. In: Presented at the 22nd Numerical Towing Tank Symposium (NuTTS 2019). Tomar, Portugal.
Vantorre, M., Verzhbitskaya, E., Laforce, E., 2002. Model test based formulations of ship-ship interaction forces. Ship Technol. Res. 49, 124–141.
Weintrit, A., 2013. Prioritized main potential solutions for the e-navigation concept. TransNav, the International Journal on Marine Navigation and Safety of Sea Transportation 7, 27–38. https://doi.org/10.12716/1001.07.01.03.
Weintrit, A., 2009. The Electronic Chart Display and Information System (ECDIS): an Operational Handbook. CRC Press, Boca Raton.
Wójcik, A., Hatłas, P., Pietrzykowski, Z., 2016. Modeling communication processes in maritime transport using computing with words. Archives of Transport System Telematics 9, 47–51.
Yuan, Z.-M., He, S., Kellett, P., Incecik, A., Turan, O., Boulougouris, E., 2015. Ship-to-Ship interaction during overtaking operation in shallow water. J. Ship Res. 59, 172–187. https://doi.org/10.5957/JOSR.59.3.150004.
Zhao-lin, W., 1988. Analysis of radar PAD information and a suggestion to reshape the PAD. J. Navig. 41, 124–129.